Prediction of (n, γ) cross sections for weak s-component in statistical model with a microscopic optical potential

Saumi Dutta,* G. Gangopadhyay, and Abhijit Bhattacharyya
Department of Physics, University of Calcutta,
92, Acharya Prafulla Chandra Road, Kolkata-700009, India

Introduction

Slow neutron capture process or s-process produces about half of the heavy elements beyond iron along the valley of nuclear stability. The weak component of s-process that occurs mostly in massive stars is ascribed to the mass region $56 < A < 100$. The neutron exposure for weak component is not sufficient enough to produce nuclei to their saturation abundances and hence, the local approximation, that is, σN_s=constant does not hold good. Hence, the abundance pattern suffers from strong propagation effects for cross section uncertainties and accurate (n, γ) cross sections are required for an analysis of elemental abundance evolution via a large and coupled network calculation. In this region, there exists a shell closure at $Z = 28$. There are a few branchpoints in the path where the rates of neutron capture and β-decay become comparable. An analysis of branching, that is crucial to the determination of various parameters for s-process environment such as stellar temperature, neutron and electron density, etc., requires the knowledge of (n, γ) cross sections. In spite of significant advancements in experimental techniques, (n, γ) cross sections for a number of important isotopes, especially for unstable short-lived nuclei are still not available. Hence, theoretical statistical model calculation remains only way to predict the unknown cross sections. We have presented radiative neutron capture cross sections from a statistical model calculation using the reaction code TALYS1.8 [1] with a microscopic optical model potential folded with target radial matter densities, obtained from relativistic-mean-field (RMF) calculations at energies appropriate for the weak s-process.

*Electronic address: sadphys_rs@caluniv.ac.in

Theoretical formalism

A microscopic optical model potential is formulated, central part of which is constructed by folding the density-dependent M3Y-Reid nucleon-nucleon interaction [2] with the radial matter densities of targets, obtained from RMF calculations [3]. The complex spin-orbit potential term is taken according to Ref. [4]. The imaginary part of the optical potential is taken identical to the real part.

The (n, γ) cross sections are calculated with this potential in statistical Hauser-Feshbach formalism. Other crucial inputs, such as, nuclear level densities and dominant E1 γ-ray strength functions are taken from latest microscopic calculations [5, 6]. Within high-temperature and high-density stellar plasma, the neutron velocities are easily thermalized. Hence, Maxwellian-averaged cross sections (MACS) are calculated by folding total cross sections with the Maxwell-Boltzmann distribution function and finally the MACS values are compared with experimental values and statistical MOST predictions [7], available in the KADoNiS database [8].

Our RMF Lagrangian is based on FSU Gold parameterization [3]. To check the reliability of our RMF calculations, charge densities are obtained by convoluting point proton densities with a standard Gaussian form factor [9]. Then, the root-mean-square (rms) charge radius values, the first moments of charge distributions, are calculated and compared with available measurements. Details are available in Refs. [10, 11, 12].

TABLE I: The rms charge radius values from RMF calculations are compared with measured values.

Nucleus	r_c (fm)		Nucleus	r_c (fm)	
	Pres.	Exp.		Pres.	Exp.
^{56}Fe	3.6936	3.7377	^{57}Fe	3.7073	3.7532
^{58}Fe	3.7211	3.7745	^{59}Co	3.7505	3.7875
^{58}Ni	3.7497	3.7757	^{60}Ni	3.7777	3.8118
^{61}Ni	3.7912	3.8225	^{62}Ni	3.8113	3.8399
^{64}Ni	3.8257	3.8572	^{63}Cu	3.8467	3.8823
^{65}Cu	3.8647	3.9022	^{64}Zn	3.8775	3.9283
^{66}Zn	3.8917	3.9491	^{67}Zn	3.8986	3.9530
^{68}Zn	3.9056	3.9658	^{70}Zn	3.9366	3.9845
^{69}Ga	3.9486	3.9973	^{71}Ga	3.9688	4.0118

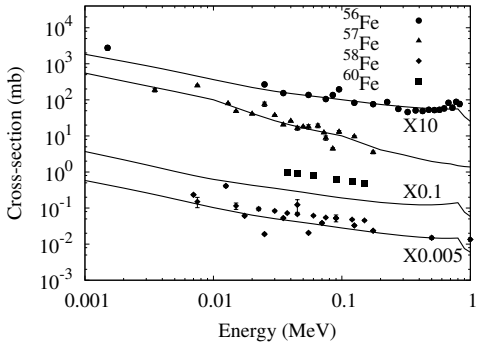

FIG. 1: Comparison of results of the present calculation (solid lines) with experimental data for $^{56-58,60}$Fe. For convenience of viewing, cross-sections for ^{56,58,60}Fe have been multiplied by a factor of 10, 0.005, 0.1, respectively.

Results

Table I shows the comparison of rms charge radius values from our calculations with available experimental data [13] for a number of nuclei in the path of the weak s-component in the neighborhood of the $Z = 28$ shell-closure. In Fig. 1, the calculated (n, γ) cross sections for the elements of iron, from 1 keV to 1 MeV, are compared with experimental values, available in the website of National Nuclear Data Center [14]. Maxwellian-averaged cross section (MACS) values at 30 keV, appropriate for classical s-process study, are listed in Table II with experimental data and theoretical MOST predictions, whenever available.

TABLE II: MACS values at $kT = 30$ keV are compared with available measurements and theoretical MOST predictions.

	MACS (mb)		
Nucleus	Pres.	Exp.	MOST
$^{56}_{26}$Fe	19.0	11.7±0.5	36.0
$^{57}_{26}$Fe	32.1	40±4	49.6
$^{58}_{26}$Fe	10.9	13.5±0.7	25.1
$^{59}_{26}$Fe	20.6		
$^{59}_{27}$Co	33.3	39.6±2.7	53.7
$^{60}_{27}$Co	46.2		
$^{58}_{28}$Ni	42.9	38.7±1.5	72.2
$^{60}_{28}$Ni	23.2	29.9±0.7	39.3
$^{61}_{28}$Ni	77.2	82±8	79.5
$^{63}_{29}$Cu	76.1	55.6±2.2	146
$^{64}_{29}$Cu	128		
$^{64}_{30}$Zn	68.8	59±5	90.9
$^{65}_{30}$Zn	250		260
$^{69}_{31}$Ga	151	139±6	122
$^{71}_{31}$Ga	121	123±8	117

Acknowledgments

Authors acknowledge the financial assistance from UGC and the AvH Foundation.

References

[1] www.talys.eu
[2] A. Kobos *et al.*, Nucl.Phys. A**384**, 65 (1982).
[3] B. G. Todd-Rutel *et al.*, Phys. Rev. Lett. **95**, 122501 (2005).
[4] R. Scheerbaum, Nucl. Phys. A**257**, 77 (1976).
[5] S. Goriely *et al.*, Phys. Rev. C **78**, 064307 (2008).
[6] S. Goriely *et al.*, Nucl. Phys. A **739**, 331 (2004).
[7] M. Arnould *et al.*, Phys. Rep. **384**, 1 (2003).
[8] www.kadonis.org
[9] A. Bouyssy *et al.*, Phys.Rev.C **36**, 380 (1987).
[10] S. Dutta *et al.*, Phys.Rev.C**93**, 024602 (2016).
[11] S. Dutta *et al.*, Phys.Rev.C**94**, 024604 (2016).
[12] S. Dutta *et al.*, Phys.Rev.C**94**, 054611 (2016).
[13] I. Angeli, ADNDT **87**, 185 (2004).
[14] www.nndc.bnl.gov